

## Supporting Information

### **Super stable giant tubes with densely packed multilayer ultrathick membranes self-assembled from purely hydrophilic polyamide**

Lipeng Wang<sup>a</sup>, Qing Zhu<sup>b</sup>, Liping Ding<sup>c</sup> and Yongping Bai<sup>a,\*</sup>

<sup>a</sup>School of Chemistry and Chemical Engineering, Harbin Institute of Technology, Harbin 150001, PR China

<sup>b</sup>Institute of chemical materials, China Academy of Engineering Physics, Mianyang 621999

<sup>c</sup>School of Chemical and Chemistry, Nantong University, Nantong, 226019, China

Corresponding author: Yongping Bai Email address: baifengbai@hit.edu.cn

Contents

#### **1. Supplemental Figures**

#### **2. Supplemental experimental procedures**

2.1 Materials

2.2 Synthesis of PASIP.400

2.3 Preparation of the PASIP.400 assembly

2.4 Instruments and measurements

2.5 Conformational stability in organic solvent

2.6 Thermal stability of autoclaved micro tubes.

2.7 Thermal Stability of the tubes under dry condition.

#### **3. Supplemental References**

## 1. Supplemental Figures

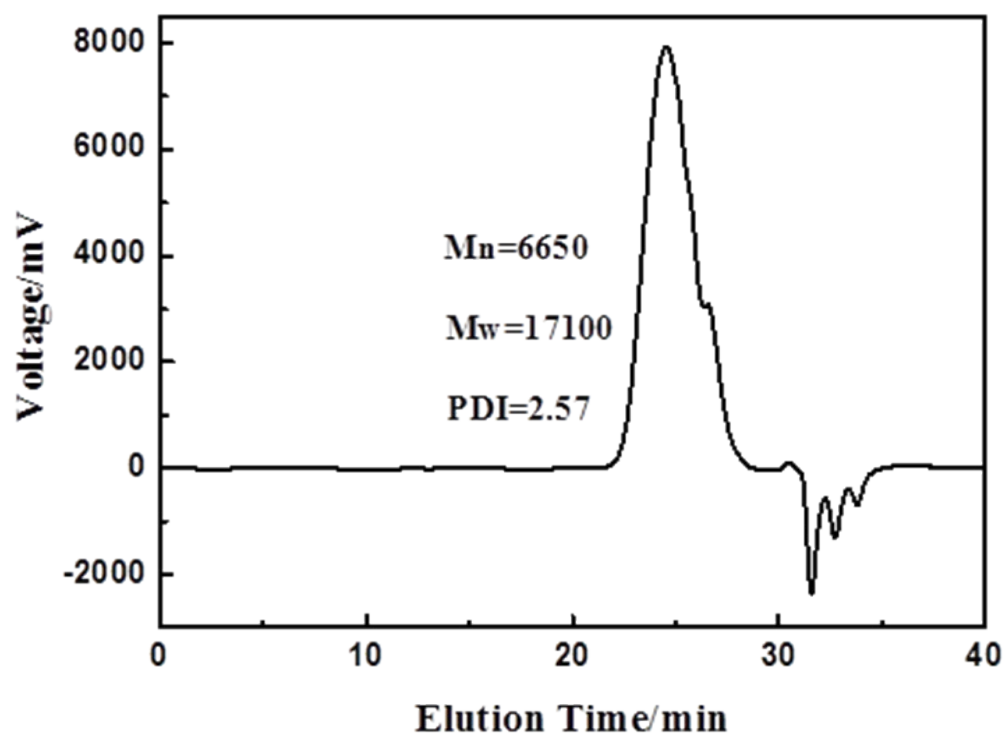
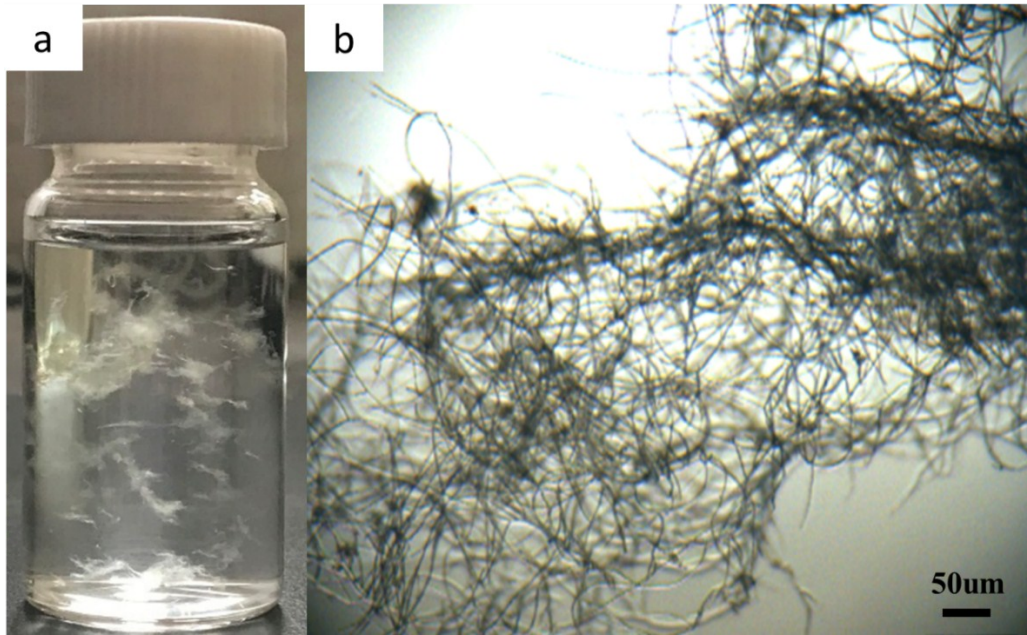
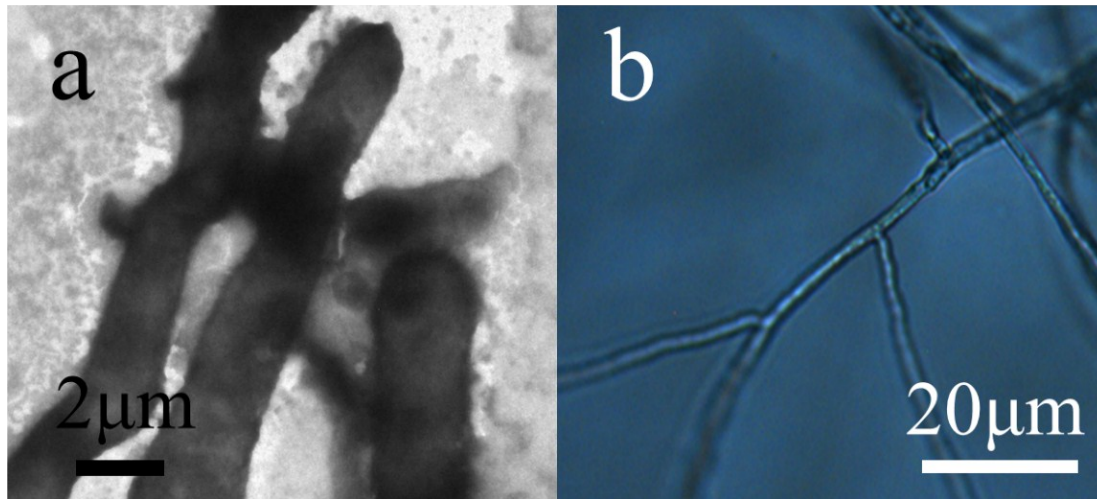


Fig.S1 GPC curve of the PASIP.400



**Fig.S2** The digital photo and OM picture of PASIP.400 assembly. (a) Digital photo of PASIP.400 assembly aqueous solution in vial. (b) OM picture of PASIP.400 assembly.



**Fig.S3** Pictures of the closed end of tubes and the Y-shaped junctions of the tubes.

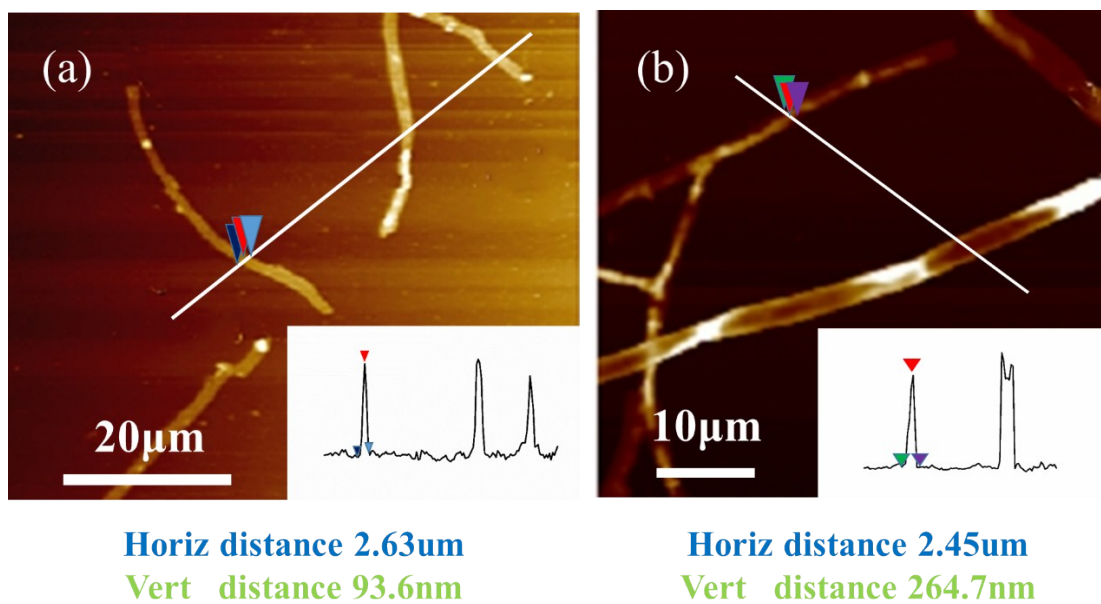


**Fig.S4** AFM image of collapsed polyamide tubes after ten days and four weeks self-assembly. (a) Ten days. (b) Four weeks. The AFM results consisted with the SEM and TEM result. The wall thickness increase with self-assembly time.

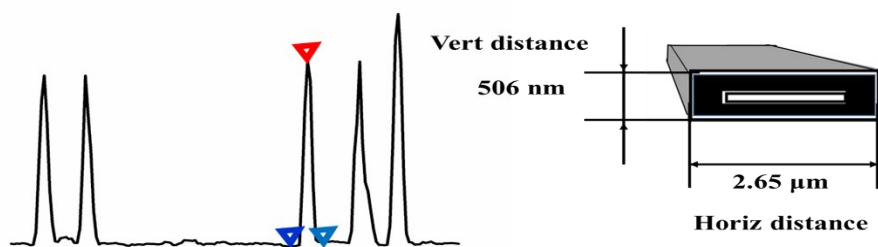
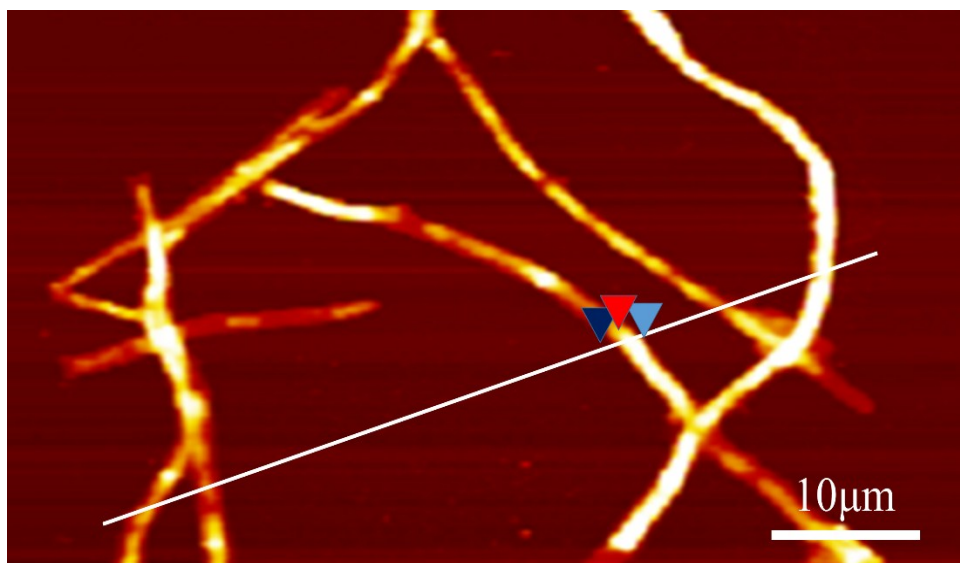


**Fig.S5** AFM image of collapsed polyamide tubes after fourteen weeks self-assembly and a representation of the structure. The AFM result showed the wall thickness reached 253nm in fourteen weeks.

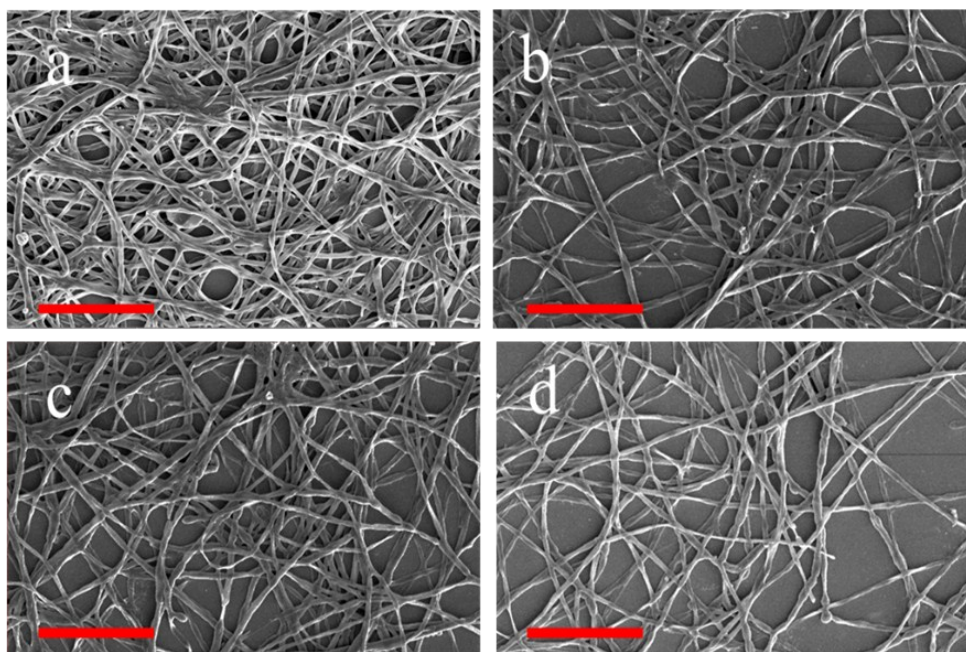


**Fig.S6** SEM images showing ultrastructure stability of the PASIP.400 tubes. Polyamides tubes after 24 hour incubation with (a) acetone, (b) NMP, (c) DMSO and (d)DMF. The scale represents 50 microns. All of these tubes treated with four different solvents present similar morphology with the untreated PASIP.400 tubes, and the length of the tubes has not changed compared, which confirmed the chemical stability of PASIP.400 tubes again.

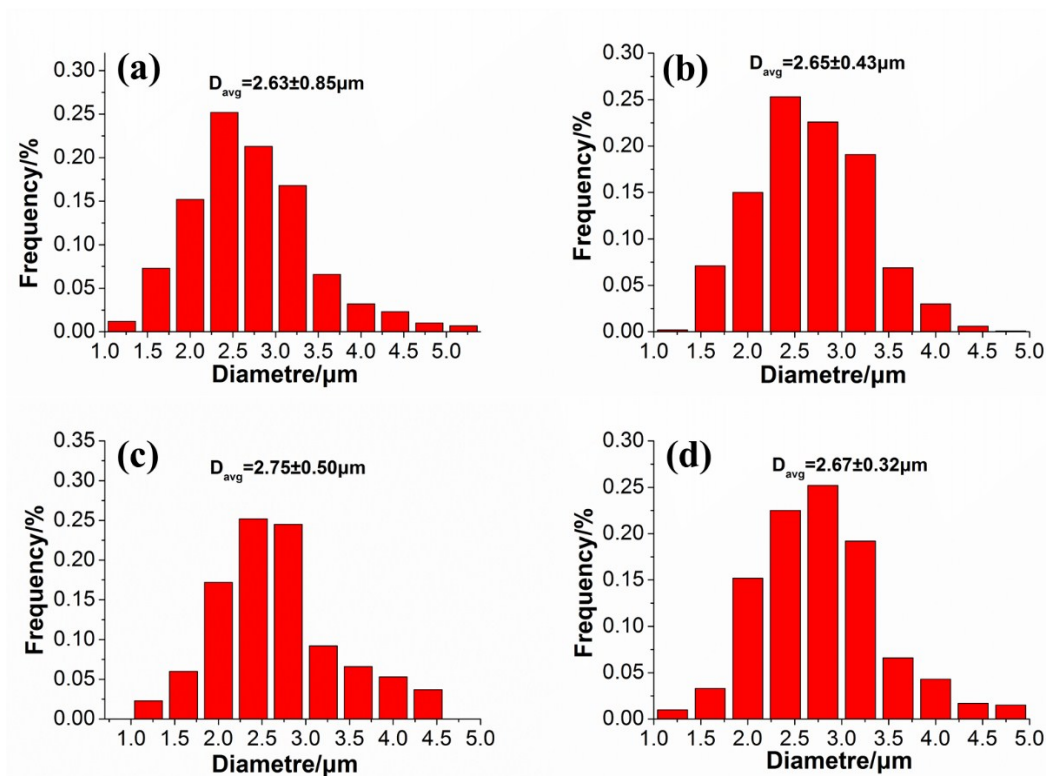


**Fig.S7** Statistical analysis on the diameter distribution of the PASIP.400 micron tubes after 24 hour incubation with (a) acetone, (b) NMP, (c) DMSO and (d)DMF. The result showed the diameters of the tubes treated by different chemical solution are about the same, which confirmed the chemical stability of PASIP.400 tubes again.

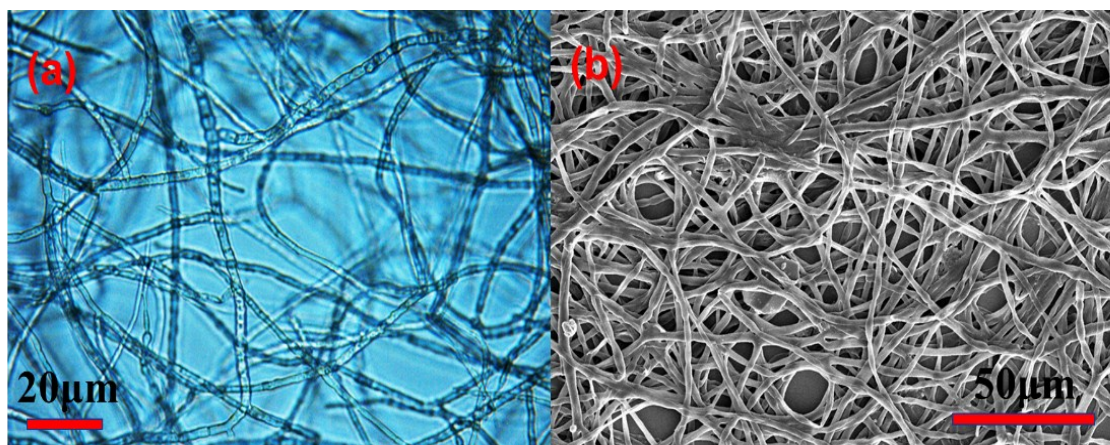


**Fig. S8** OM and SEM micrographs of autoclaved tubes (121 °C, 1.2 atm, 1h). (a) OM picture. (b) SEM picture. The length of the tubes did not decrease .

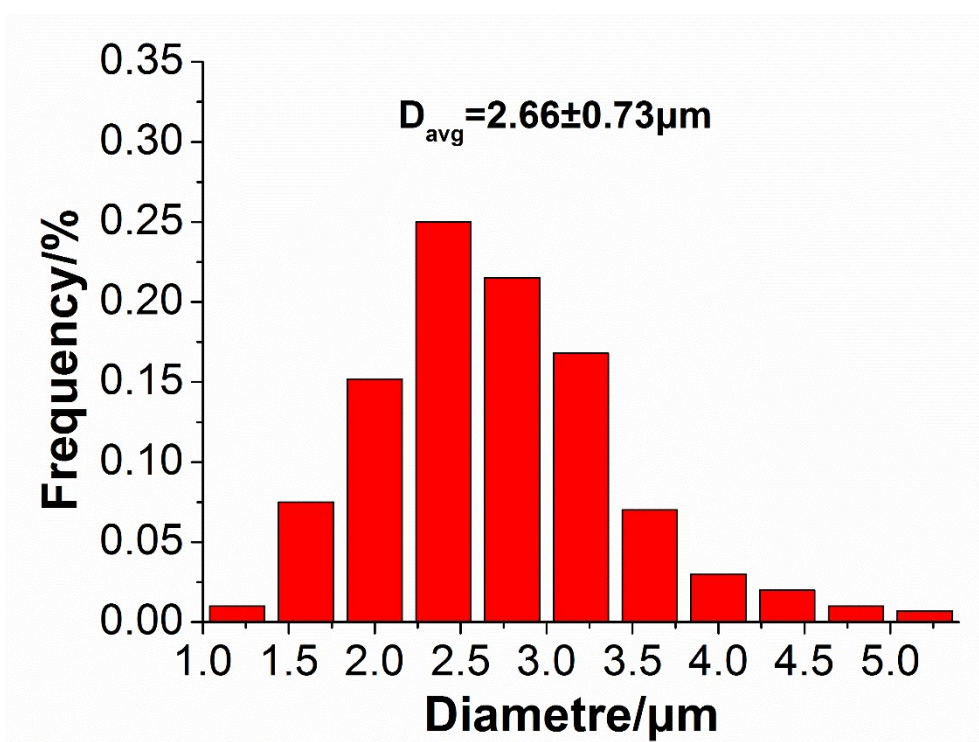


**Fig. S9** Statistical analysis on the diameter distribution of autoclaved PASIP.400 micron tubes (121 °C, 1.2 atm, 1h). The result shows that the diameter of the autoclaved tubes is inconsistent with the intact tubes

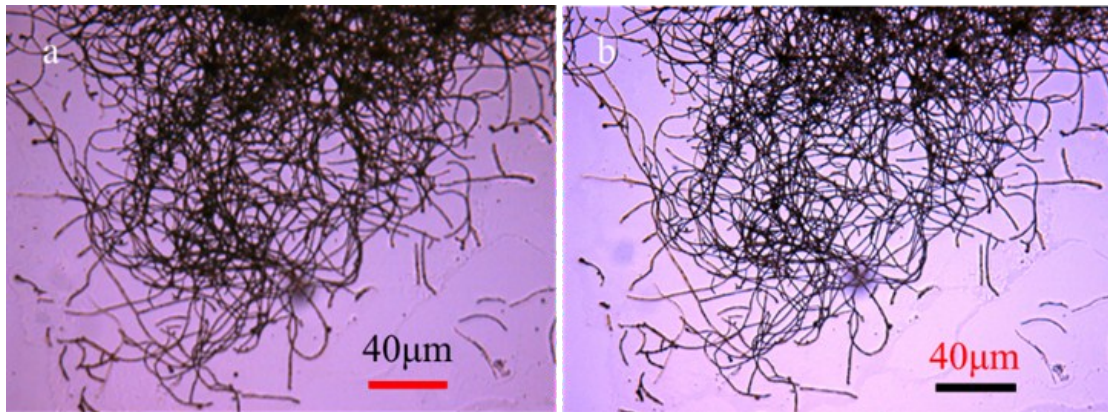


**Fig.S10** The OM picture of the micro tubes before and after 200°C heat treatment. (a) Before 200°C heat treatment. (b)After 200°C heat treatment. It can be easily found that the length and the diameter of the tubes remain the same.

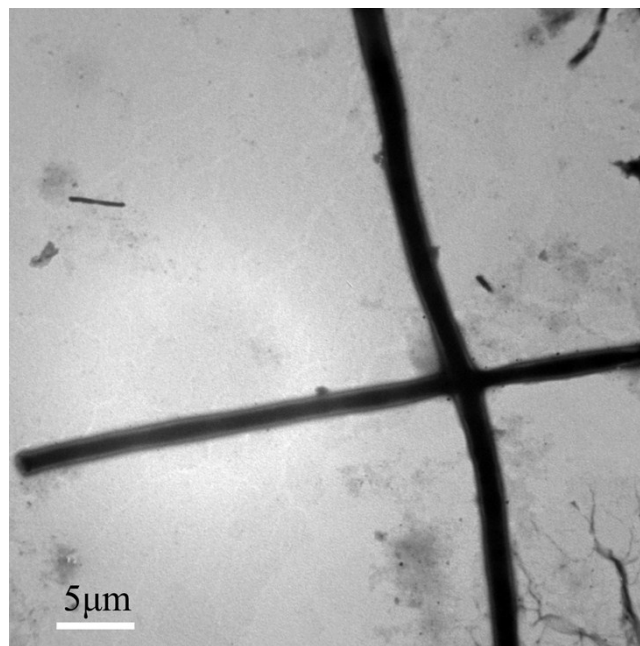


**Fig.S11** The TEM picture of the micro tubes before and after 200°C heat treatment. The hollow structure is maintained after high-temperature processing of 200°C.

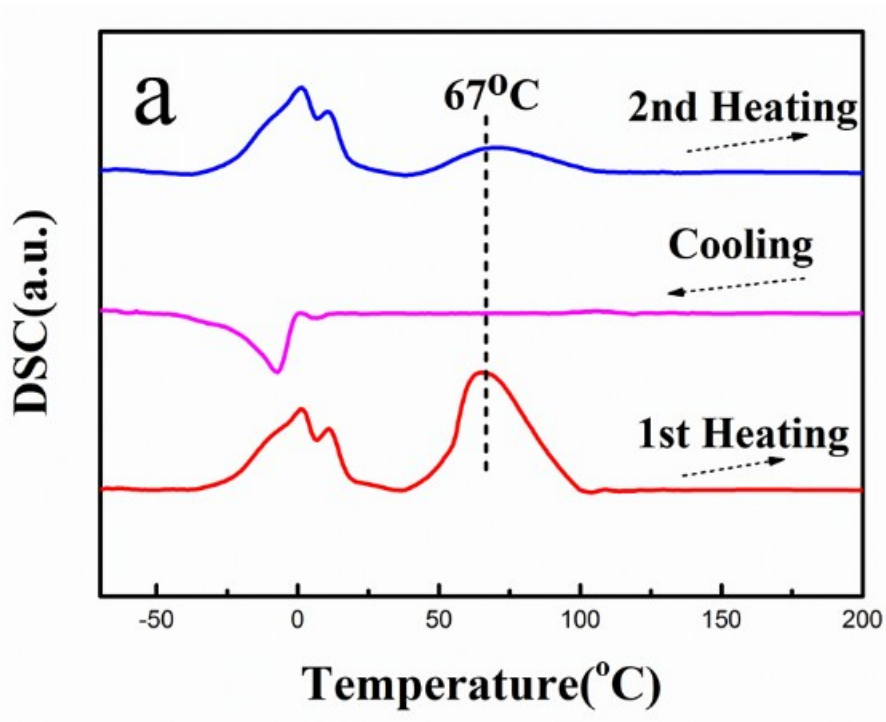


Fig. S12 DSC curves of the PATs.

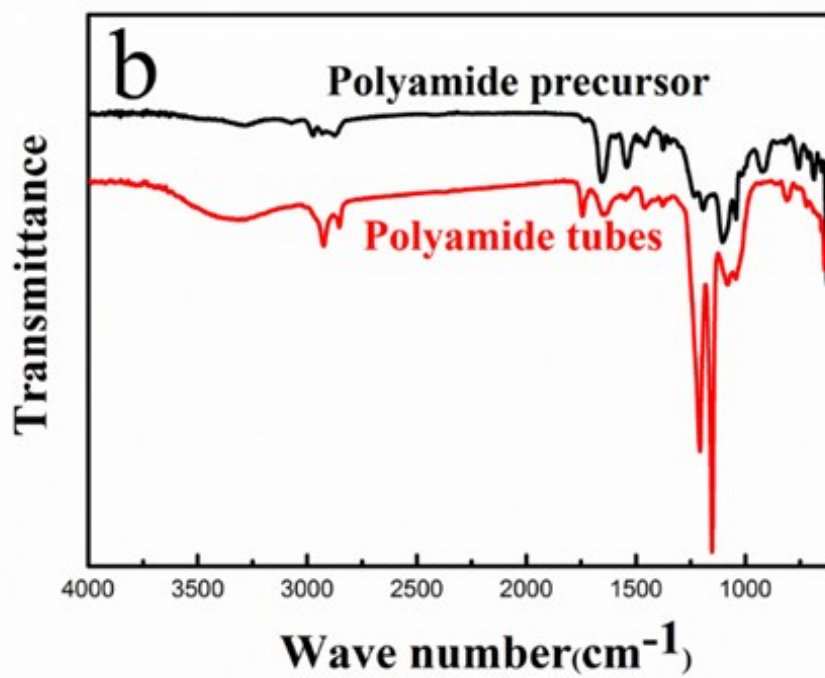
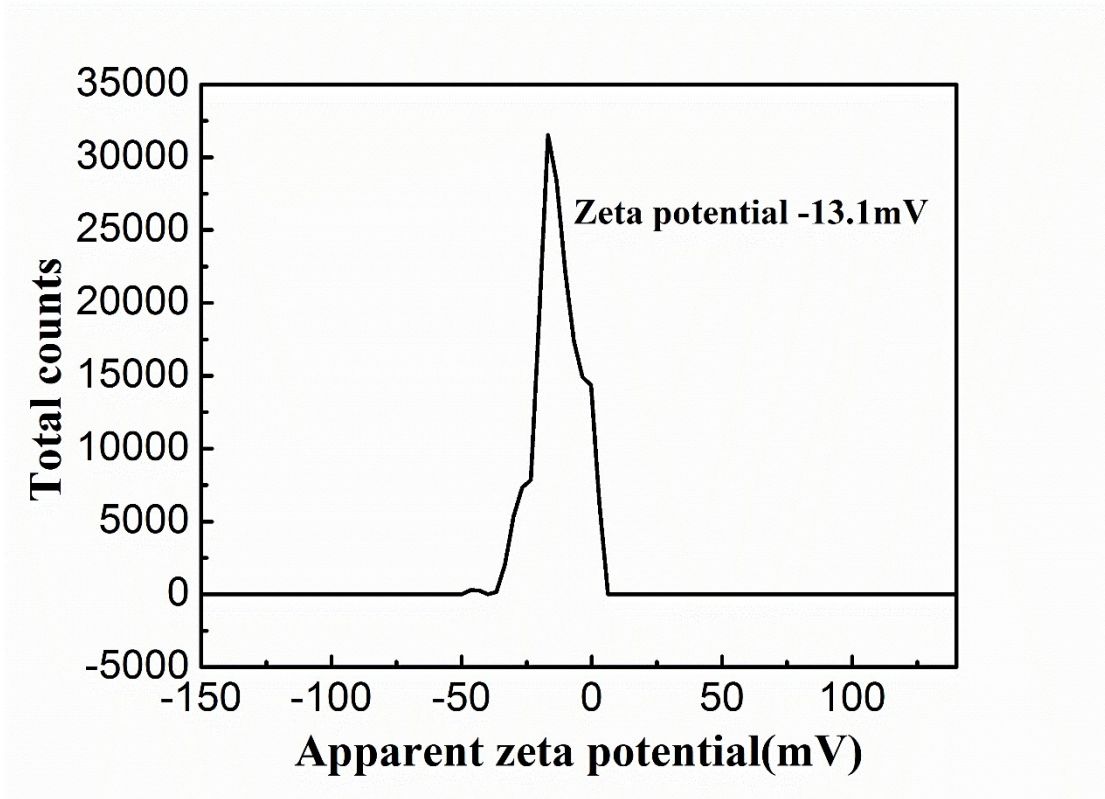
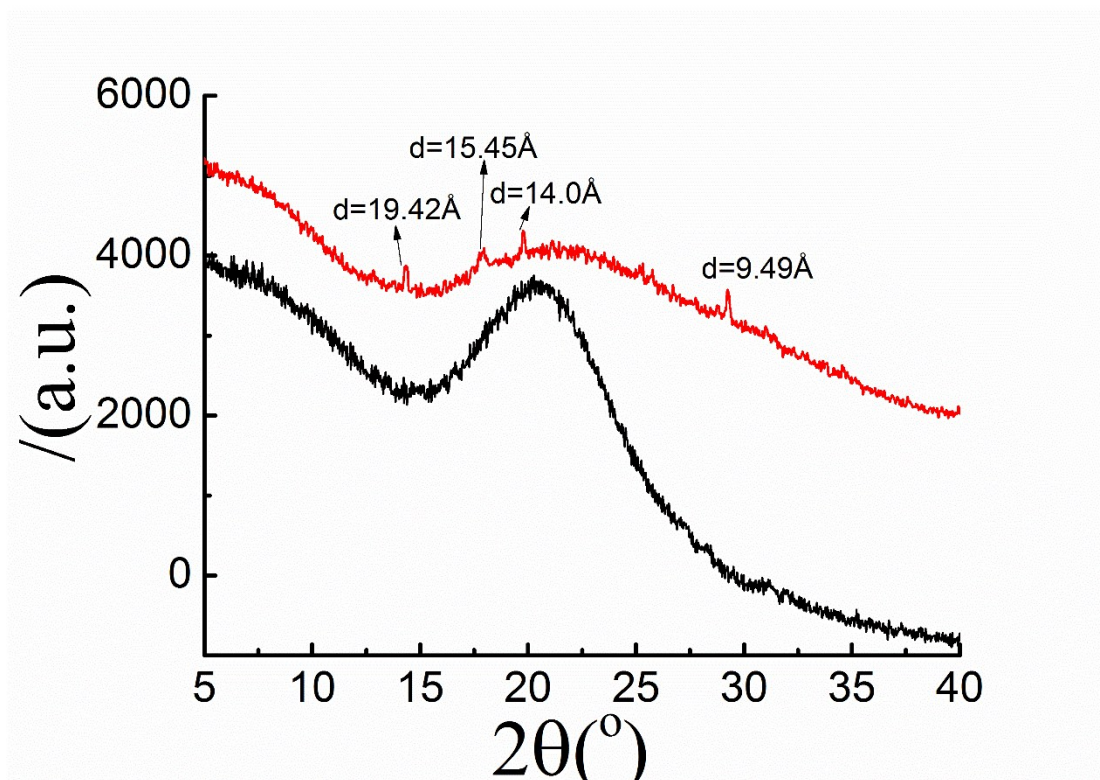


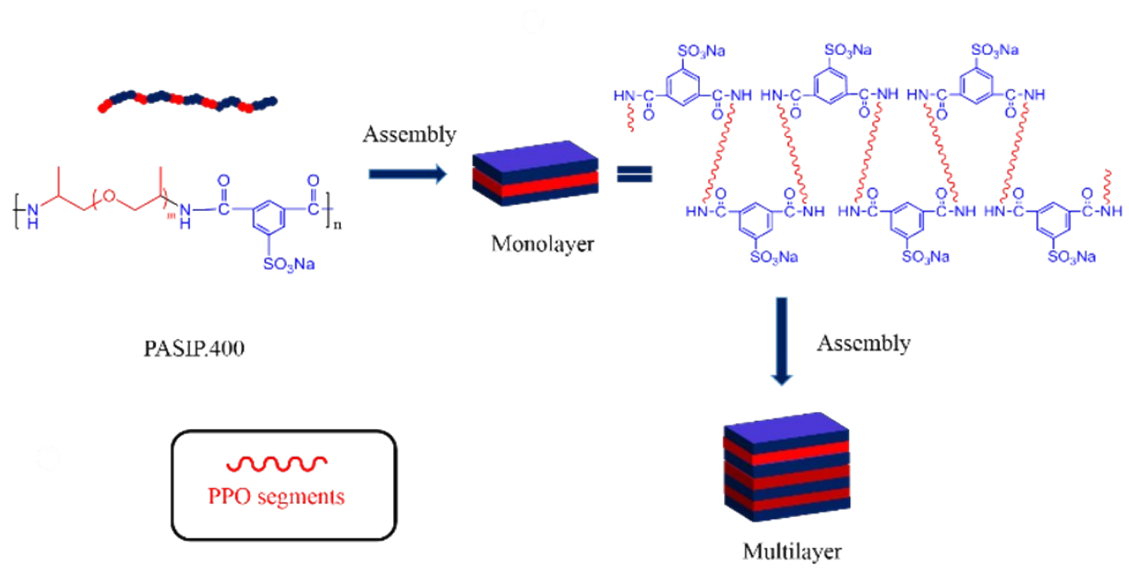
Fig. S13 FTIR spectrum of the PATs and the polyamide precursor



**Fig.S14** Zeta potential of the PASIP.400 tubes. The zeta potential of the tubes is -13.1 mV which support the outmost layer structure consist of SIPA segments.



**Fig.S15** The XRD curves of the precursor polyamide (black) and the polyamide tubes (red). Obviously, the XRD pattern shows the PASIP.400 are amorphous polymer. However, the XRD pattern of the PATs are quite complex, and several peaks assigned to specific distances were observed. The last peak is related with a distance of 0.94 nm, which agrees with the length of hydrophilic segments of SIPA. The other peaks are difficult to be assigned, which should be related with some unique packing distance of the chains in the polyamide tubes.



**Scheme S1** Proposed self-assembly mechanism of the PASIP.400

## 2. Supplemental experimental procedures

### 2.1 Materials

Poly(propylene glycol) bis(2-aminopropyl ether) ( $M_n=400,99.5\%$ ), sodium isophthalate-5-sulfonate( $99.5\%$ ), calcium chloride( $99\%$ ) and triphenyl phosphite(TPP) ( $99\%$ )were purchased from Aladdin Chemical Reagent Co., Ltd(Shanghai, China). N-methylpyrrolidinone (NMP) ( $99\%$ ), acetone ( $99\%$ ), N,N-dimethylformamide(DMF) ( $99\%$ )and dimethyl sulfoxide (DMSO) were purchased from Alfa Reagent Co. Ltd. All reagents were used as received.

### 2.2 Synthesis of PASIP.400

The polyamide PASIP.400 was synthesized by solution polycondensation in two steps following the reaction method described by Yamazaki. Flask equipped with mechanical stirrer and nitrogen inlet was charged with 2.68g of SIPA, 4g of bis (2-aminopropyl ether)-400 (Feed ratio=1:1 )and  $\text{CaCl}_2$  (18%, w/w), 7.1 mL of NMP, 1 mL of pyridine and 1.1 mL of TPP. Then, this reaction mixture was heated to  $100^\circ\text{C}$  for 3 h under  $\text{N}_2$  atmosphere. The reaction was continued for another 22 h at  $110^\circ\text{C}$  under  $\text{N}_2$  atmosphere. Finally, the polyamide solution was precipitated in 200mL of methanol. The fibrous product obtained was collected by filtration and then washed several times with acetone. The polyamide as obtained was dried in a vacuum oven at  $100^\circ\text{C}$  for 24 h.

### 2.3 Preparation of the PASIP.400 assembly

The PASIP.400 polymer were dissolved in double distilled  $\text{H}_2\text{O}$  to a final concentration of 2mg/mL to obtain a completely colorless transparent stock solution. After standing

for two weeks, the floc assembly appeared.

#### **2.4 Instruments and measurements**

Fourier Transform Infrared Spectroscopy (FT-IR) measurements were carried out on a Nicolet-Nexus 670 FT-IR in the range of 500–4500  $\text{cm}^{-1}$  with an accuracy of 16  $\text{cm}^{-1}$ . The Bruker AV-400 spectrometer was used to obtain  $^1\text{H}$  NMR spectra (400 MHz) with dimethyl sulfoxide (DMSO) used as solvent at 25 °C. GPC measurement was carried out at 25°C on a Agilent 1260 Gel permeation chromatography with DMF as solvent at a flow rate of 0.6  $\text{mL min}^{-1}$ . The differential scanning calorimeter (DSC) traces were recorded on a German NETZSCH 204 instrument. The experiment started by heating each sample from room temperature to 250 °C at a heating rate of 10°C  $\text{min}^{-1}$ , holding at 250 °C for 5 mins to eliminate thermal history of the sample, followed by cooling to -80 °C at a rate of 10°C  $\text{min}^{-1}$ , and then reheating with a ramp rate of 10 °C  $\text{min}^{-1}$  to 250 °C. The temperature was calibrated with indium. The thermogravimetric analysis (TGA) was performed on a Perkin Elmer Q5000IR thermo balance with heating rate of 10 °C  $\text{min}^{-1}$  from 25 to 800 °C under a nitrogen atmosphere.

Transmission electron microscopy (TEM) images were obtained using JEM-2100/INCA OXFORD instrument operating at an accelerating voltage of 200 KV. The dispersed sample was dropped onto a carbon membrane support and completely dried at room temperature or freeze-dried for 48 hours before measurements. Optical images were obtained using POM (Olympus BX51-P) coupled with a computer controlled charge-coupled device camera (Olympus, Japan). AFM measurement was carried out at room temperature on a Multimode Nanoscope-III<sup>a</sup> Scanning Probe Microscope

(Digital Instruments Co., Ltd, USA) equipped with a MikroMasch silicon cantilever (NSCII, radius <10 nm, resonance frequency = 300 kHz, spring constant = 40 N m<sup>-1</sup>, vertical resolution <0.03 nm, lateral resolution <2 nm) by using the tapping mode (TM). The samples for AFM observations were prepared by depositing one drop of the tube solution onto the surface of freshly cleaved mica and drying in air at room temperature overnight before measurements. The FE-SEM measurement was carried out on a Nova NanoSEM 450 (FEI, USA) with an accelerating voltage of 5 kV. A drop of sample solution was dipped onto the silica wafer and dried at room temperature or freeze-dried for 48 hours. A thin layer of platinum (Pt) or gold (Au) was coated onto the surface of samples before characterization.

### **2.5 Conformational stability in organic solvent**

50 uL of the polyamide tube solutions (mixture of tubes and water) were added into 2mL of each of the following solvents: acetone, N-Methyl pyrrolidone(NMP), dimethyl sulfoxide(DMSO) and N,N-Dimethylformamide(DMF) and incubated at room temperature for 24 hours. For SEM analysis, an aliquot (10uL) of the incubated polyamide tubes solution was air dried on a silica wafer.

### **2.6 Thermal stability of autoclaved micro tubes.**

Polyamides tube solution was autoclaved for 1 hour at 121 °C, 1.2 atm, in HB-305M autoclave(hirayama co.,ltd. Japan), for further analysis.

### **2.7 Thermal Stability of the tubes under dry condition.**

A drop of sample solution was dipped onto a microscope slide and dried at room temperature. Then, the slide with sample was observed with POM (Olympus BX51-P)

coupled with a computer controlled charge-coupled device camera (Olympus, Japan). The morphologies of the samples in different temperature were observed by rapidly heated the sample to the 200°C for 30 min at a heating rate of 30°C/min in a Linkman T95 hot stage.

DSC measurements was also used to characterize the thermal stability of the tubes under dry condition. The experiment started by cooling the dried sample from 25 to -80 °C at a rate of 10 °C min<sup>-1</sup>, and then heating the sample from -80 °C to 200 °C at a heating rate of 10°C min<sup>-1</sup>, holding at 200 °C for 30 mins, followed by cooling to -80 °C at a rate of 10°C min<sup>-1</sup>, and then reheating with a ramp rate of 10 °C min<sup>-1</sup> to 200 °C.

## **2.8 Zeta potentials measurements**

Zeta potentials were measured on a zeta potential analyzer (Zetasizer Nano ZS90, Malvern) equipped with MPT-2 Autotitrator and 4 mW He-Ne Laser based on the techniques of Laser Doppler Electrophoresis at 25 °C.

## **2.8 Wide-Angle X-Ray Diffraction (WAXD)**

WAXD patterns were recorded on a Rigaku D/MAX-2550/PC spectrometer with Cu K $\alpha$  radiation ( $\lambda = 1.542 \text{ \AA}$ ), and the scanning rate was 2° per minute from 5° to 40° (2 $\theta$ ). The q vector values were calculated according to the equation:  $q = 4\pi\sin\theta/\lambda$ . The powder samples for XRD test were prepared by freeze-dried of the self-assembly dispersion in vacuum.

### 3. Supplemental References

- 1 J.H. Fendler, CHEM. MATER., 2001, 13,3196-3210.
- 2 J.H.M. Maurer, L. González-García, B. Reiser, I. Kanelidis and T. Kraus, NANO. LETT., 2016, 16, 2921-2925.
- 3 B Dong, T Zhou, H Zhang and CY Li, ACS NANO, 2013,7, 5192-5198.
- 4 S. H. Kim, F. Nederberg, R. Jokabs, J. P. K. Tan, K. Fukushima, A. Nelson, E. W. Meijer, Y. Y. Yang and J. L. Hedrick, Angewandte Chemie International Edition, 2009,48, 4508-4512.
- 5 J. Raez, I. Manners and M.A. Winnik, J .A.C. S., 2002, 124, 10381-10395.
- 6 X. Wang, H. Wang, D.J. Frankowski, P.G. Lam, P.M. Welch, M.A. Winnik, J. Hartmann, I. Manners, and R.J. Spontak, ADV. MATER., 2007, 19, 2279-2285.
- 7 Z. Li and G. Liu, LANGMUIR, 2003, 19, 10480-10486.
- 8 J. Grumelard, A. Taubert and W. Meier, CHEM. COMMUN., 2004 ,13, 1462-1463.
- 9 J. Chen, C. Yu, Z. Shi, S. Yu, Z. Lu, W. Jiang, M. Zhang, W. He, Y. Zhou and D. Yan, Angewandte Chemie International Edition, 2015, 54,3621-3625.
- 10 A. Rosenflanz, M. Frey, B. Endres, T. Anderson, E. Richards and C. Schardt, NATURE, 2004, 430,761-764.
- 11 E. Lee, J. Kim and M. Lee, Angewandte Chemie International Edition, 2009, c48, 3657-3660.
- 12 Z. Ahmad, M.I. Sarwar and J.E. Mark, Journal of Materials Chemistry, 1997, 7, 259-263.
- 13 Y. Li, D. Yan and X. Zhu, EUR. POLYM. J.,2001, 37, 1849-1853.
- 14 J.M. García, F.C. García, F. Serna and J.L. delaPeña, PROG. POLYM. SCI., 2010, 35, 623-686.
- 15 A. Gómez-Valdemoro, N. San-José, F.C. García, J.L. DeLaPeña, F. Serna and J.M. García, POLYM. CHEM., 2010, 1,1291-1298.
- 16 Y. Ohsedo, M. Oonob, K. Saruhashib and H. Watanabeab, RSC ADV., 2015, 5, 82772-82776.

- 17 L. Wang, Q. Zhu and Y. Bai, POLYMER, 2019, 179, 121634.
- 18 Y. Bai, L. Huang, T. Huang, J. Long and Y. Zhou, POLYMER, 2013, 54, 4171-4176.
- 19 N. Yamazaki and F. Higashi, Journal of Polymer Science: Polymer Letters Edition, 1974, 12,185-191.
- 20 N. Kannan and S. Vishveshwara, Protein Engineering, 2000, 13,753-761.
- 21 N. Kol, L. Adler-Abramovich, D. Barlam, R.Z. Shneck, E. Gazit and I. Rousso, NANO LETT., 2005, 5, 1343-1346.
- 22 L. Adler-Abramovich, M. Reches, V.L. Sedman, S. Allen, S.J.B. Tandler and E. Gazit, LANGMUIR, 2006, 22, 1313-1320.
- 23c B.T. Nguyen, W. Wang, B.R. Saunders, L. Benyahia and T. Nicolai, LANGMUIR, 2015, 31, 3605-3611.
- 24 A. Blanazs, N.J. Warren, A.L. Lewis, S.P. Armes and A.J. Ryan, SOFT MATTER., 2011,7, 6399-6403.
- 25 O. Casse, A. Shkilnyy, J. Linders, C. Mayer, D. Häussinger, A. Völkel, A.F. Thünemann, R. Dimova, H. Cölfen, W. Meier, H. Schlaad and A. Taubert, MACROMOLECULES, 2012, 45, 4772-4777.
- 26 A. Taubert, E. Furrer and W. Meier, CHEM COMMUN, 2004,19, 2170-2171.